

Molecular Dynamics Simulation of Galanin in Aqueous and Nonaqueous Solution[†]

Hans De Loof,* Lennart Nilsson,[‡] and Rudolf Rigler

Contribution from the Department of Medical Biophysics, Karolinska Institutet, Box 60400, S-10401 Stockholm, Sweden, and Centre for Structural Biochemistry, Karolinska Institutet, Novum, S-14157 Huddinge, Sweden. Received October 15, 1991

Abstract: In order to increase our knowledge about the 29-residue-long neuropeptide galanin, computer simulations were carried out. As is the case with many other small peptides, galanin has nearly no secondary structure in water, unlike the situation when solvated in 2,2,2-trifluoroethanol. The galanin peptide was therefore subjected to periodic boundary molecular dynamics simulations with explicit treatment of solvent. One simulation in water (220 ps) and one simulation in 2,2,2-trifluoroethanol (120 ps) were carried out. In both cases the initial conformation was the structure, in 2,2,2-trifluoroethanol, as determined with NMR techniques (Wennerberg, A. B. A.; et al. *Biochem. Biophys. Res. Commun.* **1990**, *166*, 1102-1109). A very different behavior was observed in these different environments: the peptide remained stable in 2,2,2-trifluoroethanol while in the aqueous solution progressive unfolding of the C-terminal domain took place. The stability of the peptide in 2,2,2-trifluoroethanol validates the original structure determination. In addition, as a control experiment, the simulation points to the unique role of the water molecules in promoting the unfolding of the galanin molecule. In both simulations the probability of finding *i-i+3* hydrogen bonds was increased at the helix termini. The conformational changes occurring in the H₂O simulation were studied in more detail, and ₁₀-type helices, or the presence of *i-i+3* hydrogen bonds, were detected during the unfolding. Water molecules thus replace the backbone hydrogen bonds during the unfolding, but this does not require the insertion of a "single" water molecule, as the analysis showed that different water molecules can pair up with the original atoms involved in the backbone hydrogen bond. Other observations point to the importance of side chain-side chain and side chain-main chain interactions during the unfolding process, giving each transition its specific characteristics. In conclusion these results show that molecular dynamics simulations allow, at least qualitatively, the study of solvent effects on peptide structure and folding.

Introduction

Galanin is a 29-residue-long neuropeptide with a broad spectrum of physiological activities;¹⁻³ the galanin peptide could play a role in Alzheimer disease,⁴ and it effects insulin secretion in the pancreas.⁵ It was originally isolated from the small intestine of the pig¹ and subsequently found and characterized in a number of other species.^{6,7} The amino acid sequence of human galanin was recently determined and compared to that of the pig, rat, and cow peptide.⁸

The structure of galanin in solution has been studied with the use of NMR, CD, and IR spectroscopic techniques.^{9,10} These investigations have shown that the peptide has virtually no secondary structure in aqueous solution. However, secondary structure is present in the helix promoting solvent 2,2,2-trifluoroethanol (TFE), as has been observed in many studies on other systems.¹¹⁻¹⁵ This has allowed the determination of the three-dimensional structure of the peptide through 2D NMR techniques.^{9,10} The peptide consists basically of two α -helices interrupted by a kink induced by the invariant proline residue at position 13.

In an effort to better understand the structure-determining role of the solvent, we decided to use molecular dynamics simulation methods. Computer technology has now progressed to a point where simulations of peptides and proteins with solvent become possible.¹⁶⁻²¹ Although a simulation study on cyclosporin A showed no influence of the different solvents on the backbone structure,²² three very recent reports on other systems demonstrated how peptide conformational changes in water could be studied using molecular dynamics simulations.²³⁻²⁵ Therefore, two molecular dynamics simulations of galanin with explicit treatment of solvent were carried out, one simulation in water and one in TFE. Here we document the very different behavior of the peptide in these two different environments.

Methods

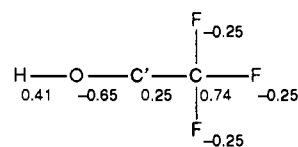
Program and Parameters. The program used for all calculations was CHARMM together with parameter set version 19.^{26,27} The polar hydrogen

* To whom correspondence should be addressed at the Department of Medical Biophysics, Karolinska Institutet.

[†] Abbreviations: NMR, nuclear magnetic resonance; CD, circular dichroism; TFE, 2,2,2-trifluoroethanol; RMSD, root mean square deviation; MD, molecular dynamics.

[‡] Centre for Structural Biochemistry, Karolinska Institutet.

Table I. Additional Parameters Used for the TFE Molecule



partial charges on the atoms

bond		
C-F	403.2 kcal/(mol Å ²)	1.39 Å
C'-C	240.0 kcal/(mol Å ²)	1.54 Å
angle		
O-C'-C	80.0 kcal/(mol-rad)	109.5°
C'-C-F	68.4 kcal/(mol-rad)	109.2°
F-C-F	77.0 kcal/(mol-rad)	109.1026°
dihedral angle		
H-O-C'-C	0.32 kcal/mol	3 (period)
O-C'-C-F	1.6 kcal/mol	3 (period)
Lennard-Jones parameter		
F	-0.109 kcal/mol	1.470 00 Å

model was used, thus explicitly treating the hydrogen atoms involved in hydrogen bonding. The covalent bonds of these hydrogen atoms were

(1) Tatemoto, K.; Rokaeus, A.; Jornvall, H.; McDonald, T. J.; Mutt, V. *FEBS Lett.* **1983**, *164*, 124-128.

(2) Rattan, S. *Gastroenterology* **1991**, *100*, 1762-1768.

(3) Rokaeus, A. *Trends Neurosci.* **1987**, *10*, 158-164.

(4) Hokfelt, T.; Millhorn, D.; Seroogy, K.; Tsuruo, Y.; Ceccatelli, S.; Lindh, B.; Meister, B.; Melander, T.; Schalling, M.; Bartfai, T.; Terenius, L. *Experientia* **1987**, *43*, 768-780.

(5) McDonald, T. J.; Dupre, J.; Tatemoto, K.; Greenberg, G. R.; Radziuk, J.; Mutt, V. *Diabetes* **1985**, *24*, 192-196.

(6) Vrontakist, M. E.; Peden, L. M.; Duckworth, M. L.; Friesen, H. G. *J. Biol. Chem.* **1987**, *262*, 16755-16758.

(7) Rokaeus, A.; Carlquist, M. *FEBS Lett.* **1988**, *234*, 400-406.

(8) Bersani, M.; Johnsen, A. H.; Hojrup, P.; Dunning, B. E.; Andreasen, D. J.; Holst, J. J. *FEBS Lett.* **1991**, *283*, 189-194.

(9) Wennerberg, A. B. A.; Cooke, R. M.; Carlquist, M.; Rigler, R.; Campbell, I. D. *Biochem. Biophys. Res. Commun.* **1990**, *166*, 1102-1109.

(10) Rigler, R.; Wennerberg, A. B. A.; Cooke, R. M.; Elofsson, A.; Nilsson, L.; Vogel, H.; Holley, L. H.; Carlquist, M.; Langel, U.; Bartfai, T.; Campbell, I. D. *Galanin*; Hokfelt, T., Bartfai, T., Eds.; Macmillan: New York, 1991.

(11) Nelson, J. W.; Kallenbach, N. R. *Proteins* **1986**, *1*, 211-217.

(12) Lehrman, S. R.; Tuls, J. L.; Lund, M. *Biochemistry* **1990**, *29*, 5590-5596.

constrained with the SHAKE algorithm (tolerance 0.0001 Å), and a 1-fs time step was used. The nonbonded distance cutoff was set to 13 Å, as recent calculations have shown the importance of using a relatively long cutoff distance.²⁸ The electrostatic term was shifted while the van der Waals term was switched between 9.5 and 13 Å. The nonbonded list was updated every 10 steps.

The rigid TIP3P water model²⁹ was used to simulate the water molecules. The parameters for 2,2,2-trifluoroethanol, based on values reported in the literature for similar components,^{30–32} are given in Table I.

Coordinate Setup. The rat galatin peptide was acetylated at the N-terminal end and was simulated in the C-terminal amidated form, a characteristic feature of many neuropeptides.³³ This results in a peptide with no overall charge, and therefore no counterions had to be introduced into the simulation system. The sequence of rat galatin is the following: Gly-Trp-Thr-Leu-Asn-Ser-Ala-Gly-Tyr-Leu-Leu-Gly-Pro-His-Ala-Ile-Asp-Asn-His-Arg-Ser-Phe-Ser-Gly-Lys-His-Gly-Leu-Thr-NH₂.

The starting conformation of the rat galatin peptide was a structure as obtained from the NMR experiments in TFE (ref 9 and Wennerberg, A. B. A.; et al. Personal communication). Although the total amount and precision of the NMR data may not yet be sufficient to exactly locate the position of every side chain, the basic structure of the peptide, two α -helices interrupted by a kink, was independent of the structure-generating procedure. This structure was extensively minimized in vacuum. Periodic boundary conditions were used to solvate the peptide, using the image facility in the CHARMM program.²⁶ The box consisted of a hexagonally shaped prism, with a long axis of 55 Å and a total volume of 42 868 Å³. This cell was filled with 1428 H₂O molecules or 351 TFE molecules using an equilibrated cubic box of solvent as a building block. Subsequently the galatin molecule was centered along the long axis of the box, and a number of solvent molecules were eliminated, corresponding to the volume of the peptide. The peptide volume was calculated from the residue-volume data compiled by Perkins.³⁴ This approach is a compromise between using the volumes from single amino acid crystals, where no hydration is taken into account, and using the volumes from densitometric measurements where the protein volume may be overestimated.³⁴ All water molecules with any atom closer than 1.65 Å to any of the peptide atoms were thus eliminated, leaving a total of 1296 water molecules in the system. For the TFE simulation, 319 solvent molecules were used, after eliminating 21 TFE molecules to create the same volume for the peptide. It should be noted that the methods, described in the literature, for eliminating the excess solvent during the setup of molecular dynamics simulations differ substantially: here 132

(13) Bradley, E. K.; Thomason, J. F.; Cohen, F. E.; Kosen, P. A.; Kuntz, I. D. *J. Mol. Biol.* **1990**, *215*, 607–622.

(14) Bruch, M. D.; Dhingra, M. M.; Gierash, L. M. *Proteins* **1991**, *10*, 130–139.

(15) Dyson, H. J.; Wright, P. E. *Annu. Rev. Biophys. Biophys. Chem.* **1991**, *20*, 519–538.

(16) Berendsen, H. J.; van Gunsteren, W. F.; Zwinderman, H. R. J.; Geursten, R. G. *Ann. N.Y. Acad. Sci.* **1986**, *482*, 269–286.

(17) Levitt, M.; Sharon, R. *Proc. Natl. Acad. Sci. U.S.A.* **1988**, *85*, 7557–7561.

(18) Aqvist, J.; Tapia, O. *Biopolymers* **1990**, *30*, 205–209.

(19) Avbelj, F.; Moul, J.; Kitson, D. H.; James, M. N. G.; Hagler, A. T. *Biochemistry* **1990**, *29*, 8658–8676.

(20) Kichen, D. B.; Hirata, F. H.; Westbrook, J. D.; Levy, R.; Kofke, D.; Yarmush, M. *J. Comput. Chem.* **1990**, *11*, 1169–1180.

(21) Tirado-Rives, J.; Jorgensen, W. L. *J. Am. Chem. Soc.* **1990**, *112*, 2773–2781.

(22) Lautz, J.; Kessler, H.; van Gunsteren, W. F.; Weber, H.-P.; Wenger, R. M. *Biopolymers* **1990**, *29*, 1669–1687.

(23) Tirado-Rives, J.; Jorgensen, W. L. *Biochemistry* **1991**, *30*, 3864–3871.

(24) DiCapua, F. M.; Swaminathan, S.; Beveridge, D. L. *J. Am. Chem. Soc.* **1990**, *112*, 6768–6771.

(25) Tobias, D. J.; Metz, J. E.; Brooks, C. L., III. *Biochemistry* **1991**, *30*, 6054–6058.

(26) Brooks, R.; Bruccoleri, R. E.; Olafson, B. D.; States, D. J.; Swaminathan, S.; Karplus, M. *J. Comput. Chem.* **1983**, *4*, 187–217.

(27) Reiher, W. E. Ph.D. Thesis, Harvard University, Cambridge, MA, 1985.

(28) Loncharich, R. J.; Brooks, B. R. *Proteins* **1989**, *6*, 32–45.

(29) Jorgensen, W. L.; Chandrasekhar, J.; Madura, J. D.; Impey, R. W.; Klein, M. L. *J. Chem. Phys.* **1989**, *79*, 926–935.

(30) Boyd, R.; Kesner, L. *J. Chem. Phys.* **1980**, *72*, 2179–2190.

(31) Clark, M.; Cramer, R. D.; Van Opdenbosch, N. *J. Comput. Chem.* **1990**, *10*, 982–1012.

(32) Bohm, H. J.; Ahlrichs, R.; Scharf, P.; Schiffer, H. *J. Chem. Phys.* **1984**, *81*, 1389–1395.

(33) Mutt, V. *Fidra Res. Award Lect.* **1989**, *3*, 125–218.

(34) Perkins, S. J. *Eur. J. Biochem.* **1986**, *157*, 169–180.

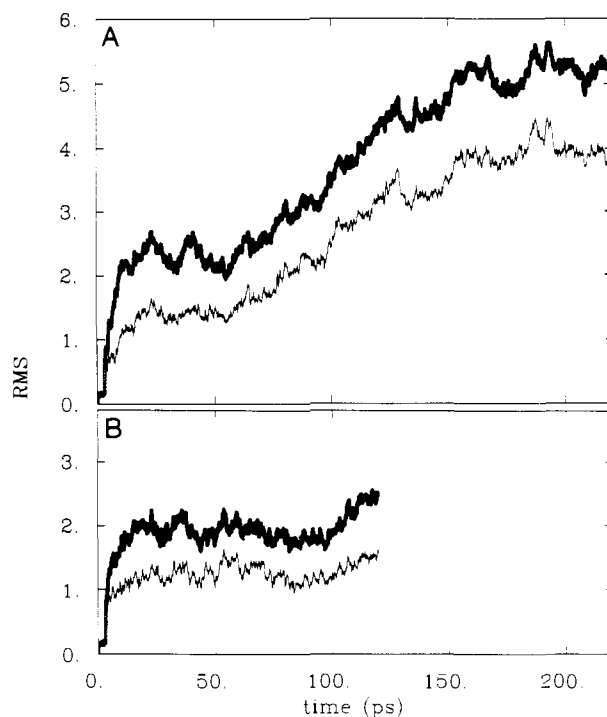


Figure 1. RMSD of the galatin peptide vs starting structure for the H₂O (A) and the TFE (B) simulations. During the simulations galatin conformations were stored every 20 fs, and subsequently compared with the starting structure. In both cases, the thick upper line is the value for the side chain atoms and the bottom line represents the values for the backbone atoms.

water molecules were replaced with the galatin molecule, while other methods would have resulted in the elimination of 116–151 molecules.^{21,16}

This setup was concluded by 100 steps of steepest descent minimization of the solvent, with the peptide harmonically constrained to its original conformation. This was done in order to eliminate remaining close contacts and unfavorable geometric strain in the system.

Molecular Dynamics Protocol. The two molecular dynamics simulations were started in exactly the same way. The peptide was harmonically constrained to its original Cartesian coordinates during the first 3 ps, enabling the solvent to further equilibrate. The complete system was gradually heated to 300 K within the first 200 fs; every 10 steps new velocities from a Maxwellian distribution were given to all the atoms. These reassignments of velocities were continued during the first picosecond. During the second picosecond new velocities were given if the average temperature of the system was outside the 290–310 K range. After the second picosecond, velocities were rescaled, instead of being reassigned, using the same criterion.

At the third picosecond the constraints on the peptide were removed while the velocities continued to be rescaled if the average temperature was outside the 290–310 K range. After the first 5 ps this was necessary only twice for the peptide in TFE simulation and once during the simulation in H₂O. The reason for this stable behavior of the MD run is the combination of a smooth nonbonded potential energy function together with the large size of the complete system.^{17,20} The total lengths of the simulations were 120 ps for the peptide in TFE simulation, referred to from now as the TFE simulation, and 220 ps for the peptide in aqueous solution, further referred to as the H₂O simulation.

Cpu Requirements. All calculations were performed on a CONVEX C-210 computer: 1 ps of the TFE simulation required 2.4 cpu hours, and 1 ps of the H₂O simulation required 5 cpu hours.

Results

Convergence Behavior. Figure 1 shows the root mean square deviations from the starting structure during both simulations, at 20-fs intervals. The constant values at the very beginning of both simulations are caused by the harmonic constraints acting on the peptide during the first 3 ps. This is followed by a rapid increase of the RMS to a value of about 1 Å. It is immediately apparent that in the H₂O simulation this value increases more and diverges further from its starting point when compared to the TFE simulation. In the H₂O simulation the RMS deviation has

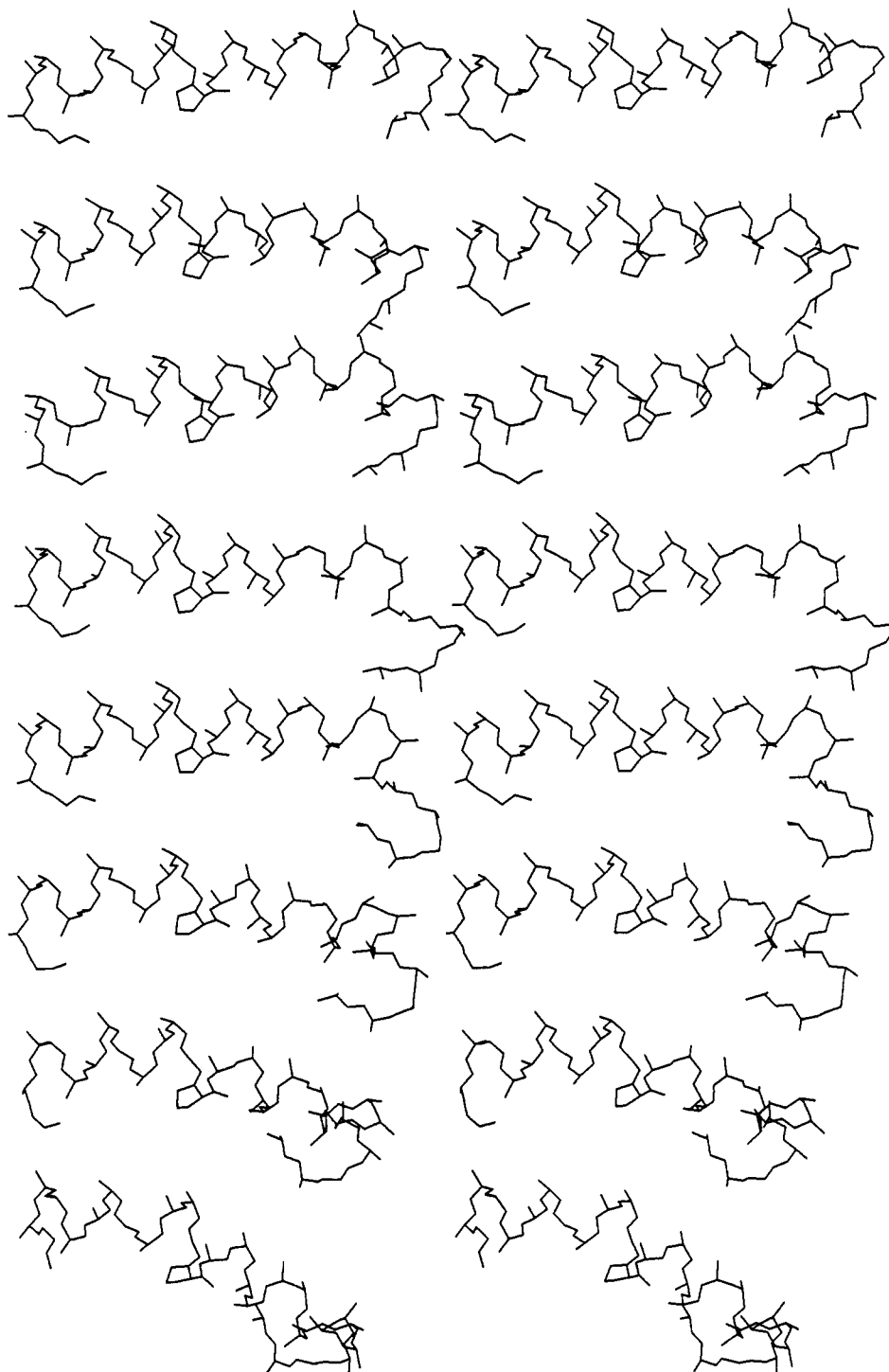


Figure 2. Stereoviews of a number of conformations, with 20-ps intervals, during the unfolding of the galanin peptide in the H₂O simulation. The structure at the top is the starting conformation.

most probably not converged after 200 ps and is likely to increase further if the simulation were to be continued. In contrast, the RMS deviation of the peptide in TFE is quite constant after the initial equilibration with the solvent, indicating its greater stability in this solvent. The plateau value for the RMS of the backbone atoms in the TFE simulations, between 1 and 1.5 Å, is similar to the values obtained during the simulations of completely solvated proteins.²¹ As is the case for most simulations of this kind, only a much longer simulation can actually prove the longevity of this state. It is however the difference in stability between these two simulations, as further documented below, which is of primary interest. These differences also prompted us to extend the H₂O simulation with an additional 100 ps, as compared to the TFE simulation. A graphical view of the events occurring during the

simulation in H₂O is shown in Figure 2.

In Figure 3 the RMS deviations per residue are shown, and this establishes what regions of the peptide are more flexible. The main difference between the two simulations is the much increased mobility of the C-terminal part of the galanin molecule in H₂O. In addition, the motions of all residues are observed to be larger during the H₂O simulation. This remains so if the H₂O simulation is analyzed as two 100-ps-long runs (data not shown). There are qualitative similarities though, such as the larger values for both extremities of the peptide as well as a small increase in the middle of the peptide, around the proline residue.

Dihedral Transitions and Fluctuations. The averages for the backbone dihedral angles together with their fluctuations are shown in Figure 4. The data in this figure further illustrate the

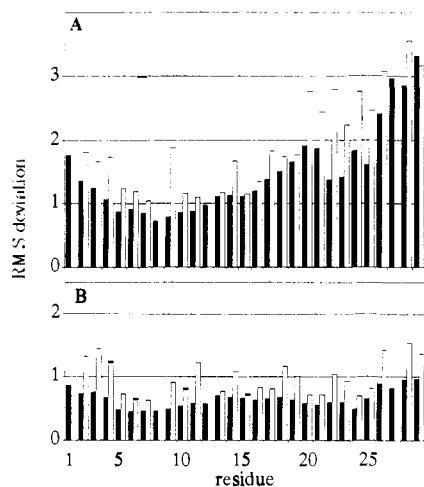


Figure 3. RMS per residue of the H₂O (A) and TFE (B) simulations. Averages were calculated of the galanin conformations during the two trajectories, excluding the first 20 ps, and the root mean square deviations for the backbone (black) and side chain (gray) atoms were determined on a residue per residue basis.

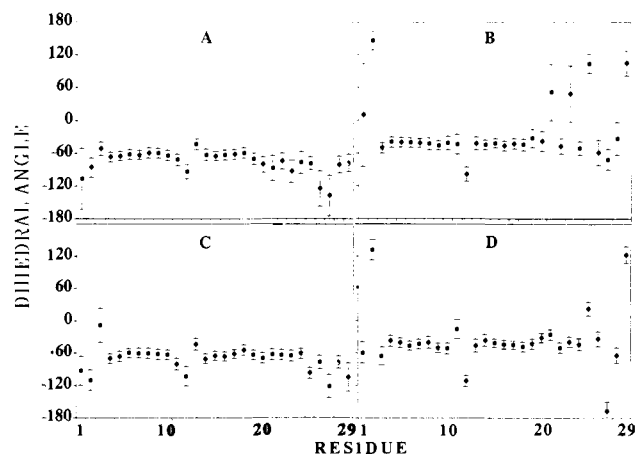


Figure 4. Averages and fluctuations for the backbone dihedral angles of the H₂O simulation (A and B) and the TFE simulation (C and D). The values for the ϕ angle are given on the right (A and C) and those for the ψ angle on the left (B and D).

differences and similarities of both MD runs. As expected, the flexibility increases at both ends of the peptide, but the values at the C-terminal end in the H₂O simulation clearly show the marks of an ongoing unfolding process. The backbone angle ψ has more dissimilarities between the two simulations. The fluctuations for the conserved helical parts and the region around the proline residue are only slightly higher in the H₂O simulation. This is probably due to the smaller size and lower mass of the H₂O molecule.

Backbone dihedral angle transitions were detected with the MONITOR facility in the CHARMM program,²⁶ and in Figure 5 these events are compared for the C-terminal end of the peptide in both MD runs. Although such an automated analysis of dihedral transitions has to be carried out with caution, due to the frequent occurrence of backbone dihedral angles not close to their minima, the comparison between the MD runs documents clearly the progressive unfolding in H₂O of the peptide in the C-terminal to N-terminal direction.

Pseudodihedral Angle Behavior. In Figure 6 the time course is shown of the values for a number of pseudodihedrals, defined by four consecutive C _{α} carbon atoms. The transitions do not seem to occur independently, and the mechanism of unfolding cannot be described by the simple sequence increase in the values of some pseudodihedrals. This is most clearly illustrated by the decrease of pseudodihedral 21 before pseudodihedral 22 starts to open. Subsequently, the value of pseudodihedral 20 increases while, at

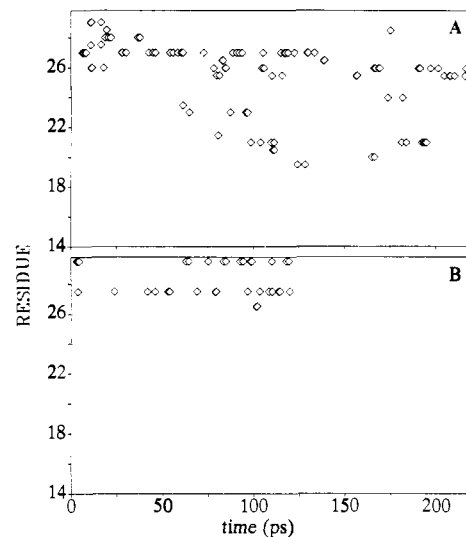


Figure 5. Dihedral transitions for the backbone angles ϕ and ψ , as determined by the MONITOR facility in the CHARMM program for the H₂O (A) and TFE (B) simulation. Note the progressive appearance, in the H₂O simulation, of transitions, from the C-terminal end toward the N-terminal end, a clear indication of the progressive unfolding of the peptide. Note also the conspicuous high number of transitions, in both cases, for residue 27, as this is a glycine residue.

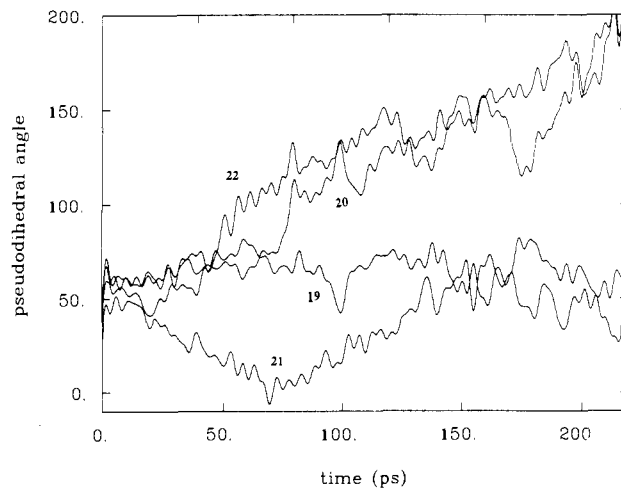


Figure 6. Evolution of the pseudodihedral angles between consecutive C _{α} carbons of the H₂O simulation. Numbers indicate the first C _{α} carbon defining the dihedral. In total four pseudodihedrals are plotted, starting from C _{α} -19 to C _{α} -23. The data were filtered for the sake of clarity so as to be able to combine all data on one graph. This was done by eliminating the high frequency part of a Fourier transform of the data.

the same time, pseudodihedral 21 reverses its trend and also becomes more extended.

Intra-peptide Hydrogen Bonds. As hydrogen bonding is most certainly a major factor in this unfolding process, it was studied in some more detail. A number of different criteria have been used by different groups to describe hydrogen bond formation.^{17,19,23,35-37} To compare some of these methods, data were compiled from a stable part of the helix in the H₂O simulation; i.e., the different criteria were applied on the possible $i-i+4$ and $i-i+3$ hydrogen bonds with the carbonyl oxygen on residue 17 as the hydrogen bond acceptor. In Table II the percentages are given of 2200 coordinate sets, sampled every 100 fs, that fit the different criteria, together with an estimate of the overlap. As expected, these numbers vary, and there is also some difference in the discriminating power of these criteria. One of the simpler

(35) Aqvist, J.; van Gunsteren, W. F.; Lijonmarck, M.; Tapia, O. *J. Mol. Biol.* **1985**, *183*, 461-477.

(36) Sundaralingam, M.; Sekharudu, Y. C. *Science* **1989**, *244*, 1333-1337.

(37) Gray, T. M.; Matthews, B. W. *J. Mol. Biol.* **1984**, *175*, 75-81.

Table II. Comparison between Hydrogen-Bonding Criteria

criterion	<i>i-i+4</i> (%)	<i>i-i+3</i> (%)	overlap ^a (%)	ref
O-H < 2.4 Å	84.1	19.6	89.1	19
O-H < 2.6 Å	78.5	35.8	81.6	17
O-N-H < 35°				
O-H < 2.5 Å	85.3	22.1	88.2	23
N-H-O > 120°				
O-H < 2.4 Å	68.9	10.1	71.1	35
N-H-O > 135°				
O-N < 3.4 Å	91.8	58.8	98.1	36
N-H-O > 90°				
O-N < 3.4 Å	91.7	59.4	97.9	37

^aOverlap is the percent of the *i-i+3* hydrogen bonds that are also *i-i+4* hydrogen bonds.

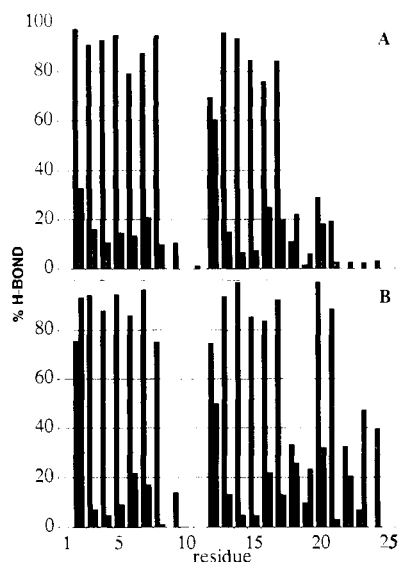


Figure 7. Percentage occupation of the main chain hydrogen bonds, both *i-i+4* (black) and *i-i+3* (gray), during both simulations. Data are compiled from 2200 and 1200 coordinate sets, saved every 100 fs, of the H₂O (A) and TFE (B) simulations, respectively.

methods, the acceptor-hydrogen distance being smaller than 2.4 Å,¹⁹ gives average results. When examined graphically (data not shown) a correlation was found between these simple criteria, the acceptor-hydrogen distance and the angle defined by the acceptor-hydrogen-donor atoms. In contrast, for the more popular acceptor-donor distance criterion, this correlation is largely absent, explaining why the additional angle measure is needed. As a single criterion is more convenient and as it simplifies the comparison between alternative hydrogen bonds, it was used in the analysis that follows. There is however not a "best" criterion, and the values obtained should only be used as relative indicators of hydrogen bond stability.

In Figure 7 the percentage occupations of main chain hydrogen bonds are given. In both simulations the helix in the N-terminal part of the molecule is quite stable and results in very similar main chain hydrogen bond formation. Also apparent is the increased frequency of *i-i+3* hydrogen bonds at the ends of both helices in both simulations. The differences between the two simulations are again most prominent at the C-terminal part of the peptide where during the H₂O simulation *i-i+4* and *i-i+3* hydrogen bonds are replaced by hydrogen bonds with the solvent.

Because of the proline residue, at position 13, three possible *i-i+4* hydrogen bonds are absent. This absence of hydrogen bonds gives additional flexibility to the molecule, and in Figure 8 the motion between the stable helical parts of the molecule are shown. This angle is defined by the axis of two cylinders fitted to the backbone atoms of residues 4-10 and 13-19. When these calculations were repeated with residues 4-13 and 12-21, nearly identical results were obtained, confirming the global nature of these motions. As three hydrogen bonds are not present this conformation is not directly comparable with the minimum

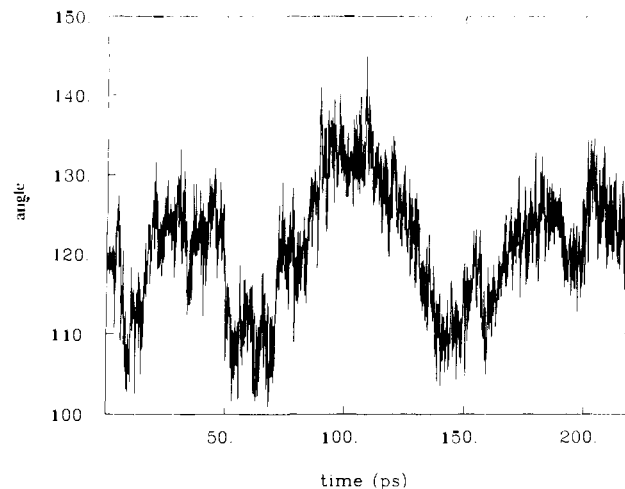


Figure 8. Evolution, during the simulation in H₂O, of the angle between the two stable helices within the galanin peptide, encompassing residues 4-10 and 13-19, respectively.

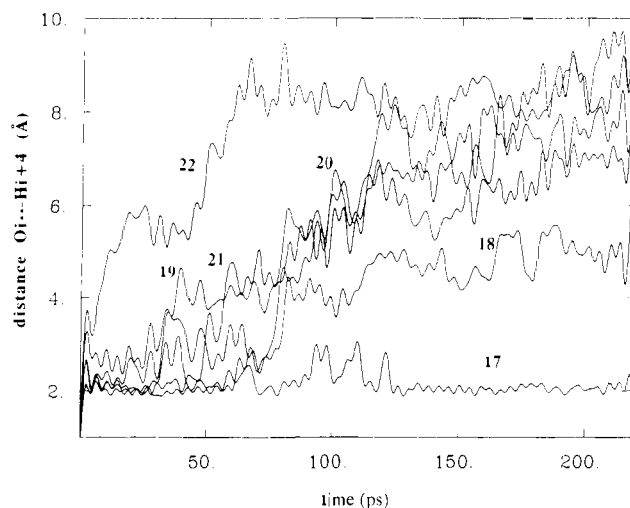


Figure 9. Oxygen(*i*)-hydrogen(*i+4*) distances for six neighboring backbone oxygen atoms starting at residue 17 of the H₂O simulation. Data points, collected every 100 fs, were filtered as in Figure 6.

perturbation of helices by a proline residue as observed in certain protein structures.^{38,39} It was not possible to detect similar slow frequency motions in the TFE simulation, and this is probably also caused by the different hydrodynamic characteristics of this solvent.

The breaking of these backbone hydrogen bonds in the C-terminal part of the galanin peptide is further documented in Figure 9. The *i-i+4* oxygen-hydrogen distances were saved every 100 fs and plotted after filtering out the high frequency "noise". As already apparent from the pseudodihedrals in Figure 6, unfolding proceeds, on average, from the C-terminal end toward the N-terminal end; i.e., the distance from the carbonyl oxygen on residue 22 increases first. This trend is however not uniform, and the His19-Ser23 hydrogen bond distance clearly increases earlier than those distances located more toward the C-terminal end. A closer inspection of what kind of residues are involved gives some clues about the origin of this sequence of events. The salt bridge side chain-side chain interaction between Arg20 and Asp24 provides the additional stability to the backbone hydrogen bond. This interaction probably also shields the hydrogen bond from attack by water molecules. In contrast, the side chain of His19 is interacting with the carbonyl oxygen of Ala15, located on the previous turn, therefore leaving plenty of room for the water

(38) Barlow, D. J.; Thornton, J. M. *J. Mol. Biol.* **1988**, *201*, 601-619.

(39) Sankaramakrishnan, R.; Vishveshwara, S. *Biopolymers* **1990**, *30*, 287-298.

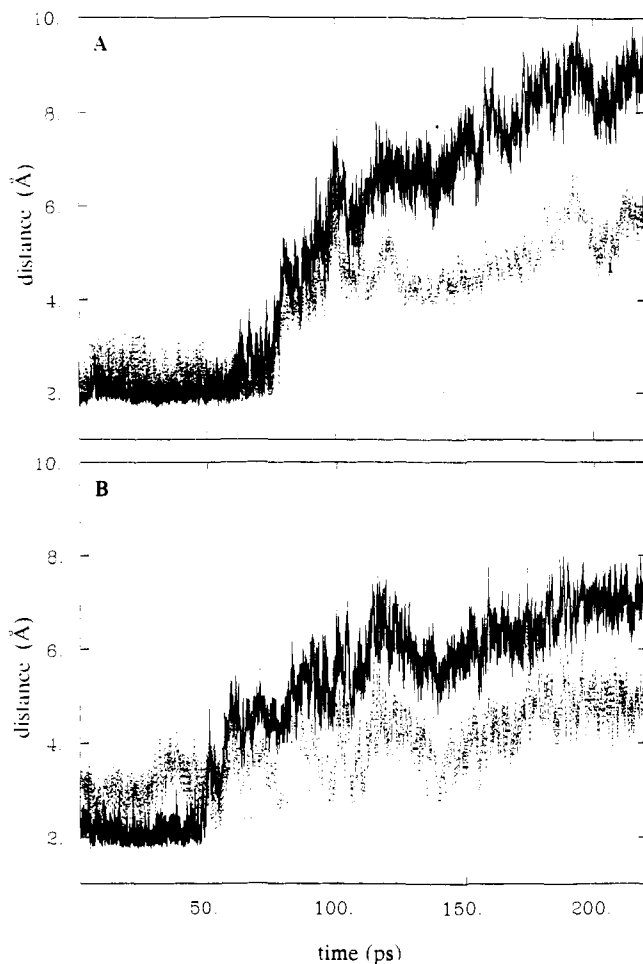


Figure 10. Time development, during the H_2O simulation, of the $i-i+4$ (solid line) and $i-i+3$ (dotted line) hydrogen bond distances for two consecutive residues: Arg20 (A) and Ser21 (B). Note the transiently lower distances for the $i-i+3$ hydrogen bonds when the unfolding of the peptide starts. Data points are the instantaneous values at 20-fs intervals, and in contrast to Figure 9, the data were not filtered.

molecules to attack the His19–Ser23 hydrogen bond first. (More on water–peptide interactions follows below.) After 220 ps the hydrogen bond between the oxygen on residue 17 and the hydrogen on residue 21 is still intact, and much longer simulations would be needed to determine how or if unfolding would proceed.

The increased occurrence, on average, of $i-i+3$ hydrogen bonds at the end of the helices was described in Figure 7, and therefore the presence, during the unfolding process, of this alternative hydrogen bonding pattern was further investigated. A role for this $i-i+3$ hydrogen bonding during the folding of α -helices was recently proposed by others,^{24,25,36} and while this work was in progress, Tirado-Rives and Jorgensen²³ noted the presence of 3_{10} -type helices during the unfolding of a ribonuclease S peptide analogue in their MD simulation. Figure 10 shows the $i-i+4$ and $i-i+3$ oxygen–hydrogen distances, during two of these unfolding events. Although both transitions clearly have some individual features, there is a relatively short lived decrease of the $i-i+3$ distances during the transitions. Similar observations were made for the breaking of the Asn18–Phe22 and the His19–Ser23 hydrogen bonds, but all these transitions have individual features that may be more important than the transient occurrence of these $i-i+3$ hydrogen bonds.

Solvent–Peptide Interactions. The role of water molecules during these unfolding events was also studied. The first observations made during the analysis were local structural changes occurring during the very first picoseconds of the simulation. These small rearrangements, reflected by the initial increase of the RMS deviations in Figure 1, have two main origins: (1) the presence of the solvent molecules, as the starting conformation

was a structure minimized in vacuum, and (ii) the addition of thermal energy at the start of the MD run. For example, the polar hydrogens on the Asn18 side chain interacted with carbonyl oxygen on the Asp17 side chain or the backbone carbonyl of Ala15, but this occurred exclusively during the first 8 ps. Most of these rearrangements involved the side chains or the last two residues on either side of the peptide, and this in both simulations.

The differences between the TFE and H_2O simulations, however, reveal a dramatic effect of the solvent beyond these initial rearrangements, and the H_2O molecules are thus promoting the unfolding events described above. There is an additional interest in describing this solvent effect in more detail as a hypothesis has been put forward where, as a folding intermediate, a single water molecule is inserted as a bridge between former donor–acceptor atoms in the backbone of the α -helix.^{24,36}

Figure 11 illustrates the events developing during the breaking of four neighboring $i-i+4$ hydrogen bonds, starting with the Asn18–Phe22 bond. Hydrogen-bonding distances, at 100-fs intervals, are shown between the backbone atoms and between these and the closest water molecule. At the bottom of each plot, a 1-Å vertical line was drawn if the closest water molecule to the peptide carbonyl oxygen and to the amide hydrogen is the same molecule. If this is the case while the backbone hydrogen bond opens and the backbone–water distances decrease, a “single water insertion” event is happening. This is a more direct way of analyzing the events as compared to the sorting of distances as performed by DiCapua et al.²⁴

When an $i-i+4$ hydrogen bond breaks, it is, not unexpectedly, replaced very rapidly by a hydrogen bond with the solvent; i.e., in nearly all coordinate sets one distance is close to a hydrogen-bonding distance. Another observation recurring in all four events is that a hydrogen bond between a water molecule and the backbone carbonyl oxygen is readily formed, and that this bond can coexist with the backbone hydrogen bond for a relatively extended period of time. It is then, in general, the formation of the hydrogen bond between the amide hydrogen and the water oxygen that coincides with the opening up of the backbone hydrogen bond and ultimately the unfolding of the α -helix.

What is most dissimilar among those events is the precise role of a “single” water molecule. In Figure 11A the main unfolding event occurs around the 75-ps mark, when the water molecule approaches the backbone amide and the $i-i+4$ hydrogen bond distance increases. It is precisely at this moment that the backbone interacts with a single water molecule. The next backbone hydrogen bond, from His19 to Ser23, breaks up much earlier, as was already noticed in Figures 6 and 9. The main event occurs about 35 ps into the simulation, and from Figure 11B it becomes clear that for the next 30 ps a single water molecule is interacting with the backbone. The neighboring $i-i+4$ hydrogen bond breaks about 80 ps into the simulation (Figure 11C), and up to 20 ps before this event single water molecules are close to both backbone atoms. They do not however form a strong hydrogen bond with the peptide, and therefore different water molecules are ultimately involved in the unfolding process. The Ser21–Lys25 backbone hydrogen bond (Figure 11D) is eliminated after about 50 ps, and it is clear that different water molecules are the new hydrogen bond partners of the backbone atoms.

The analysis thus showed considerable diversity of the solvent behavior during these unfolding events, and in contrast to the hypothesis mentioned above, it is clear that the donor–acceptor atoms of a broken intrachain hydrogen bond can also pair up with different solvent molecules. Each transition seems therefore to have individual characteristics determined by its position in the chain and most probably also by the side chain–side chain interactions in its surroundings.

As already mentioned the TFE simulation is much more eventless. But, for the sake of comparison, data for the Ser21–Lys25 backbone hydrogen bond are given in Figure 12. The hydrogen bond is very stable as illustrated by the $i-i+4$ hydrogen-bonding distance (upper line). There are, as in the H_2O case, interactions between the carbonyl oxygen and the polar hydrogen on TFE. The next event necessary for unfolding, the interaction

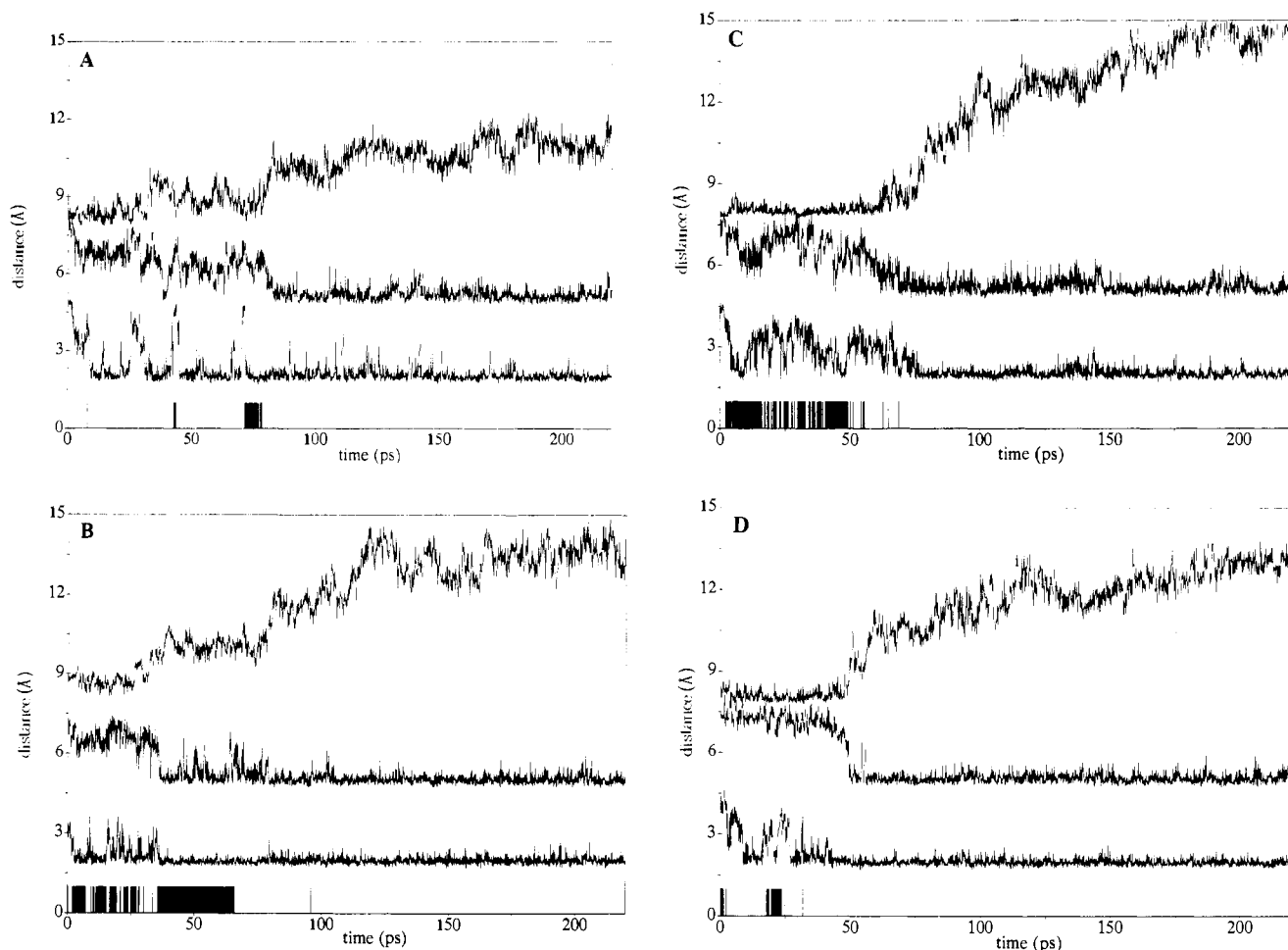


Figure 11. Time course of the hydrogen-bonding events around four consecutive $i-i+4$ hydrogen bonds that are broken during the H_2O simulation: (A) Asn18–Phe22, (B) His19–Ser23, (C) Arg20–Asp24, and (D) Ser21–Lys25. Data are shown from 2200 coordinate data sets, sampled every 100 fs. On the bottom of each plot 1-Å vertical lines are drawn if the water molecule closest to the carbonyl oxygen on residue i is the same molecule with the closest approach to the amide hydrogen on residue $i+4$. (For different coordinate sets, however, this can be a different water molecule!) In addition, three continuous data lines are present: the bottom line is the closest carbonyl oxygen–water hydrogen distance, the one above is the closest amide hydrogen–water oxygen distance, which for clarity is offset by 3 Å, and the upper most line, off set by 6 Å, is the backbone $i-i+4$ carbonyl oxygen–amide hydrogen distance.

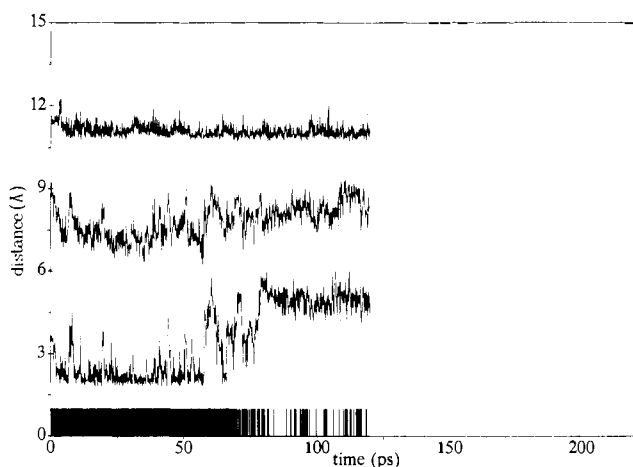


Figure 12. Data, similar to Figure 11, for the hydrogen-bonding events around the Ser21–Lys25 hydrogen bond in the TFE simulation. Note that for the clarity of the figure the upper data line was offset 9 Å, instead of 6 Å, as in Figure 11.

of the backbone amide hydrogen with the solvent, does not occur. Other $i-i+4$ hydrogen bonds in the TFE simulation have their own characteristics (data not shown), but the general behavior mentioned for the Ser21–Lys25 backbone hydrogen bond was also valid for them.

Discussion and Conclusion

The calculations in this paper document a behavior of the galanin peptide in H_2O that is in overall agreement with the fact that experimentally no secondary structure is observed in aqueous solution.^{9,10} The stability of galanin in TFE makes structure determination possible with NMR technology, and in parallel the simulations show that much of the secondary structure remains intact. This also further validates the original experimental structure determination,^{9,10} although it is not an independent proof of its correctness.

It therefore seems possible to study, in atomic detail, the behavior of a (small) peptide system and its interaction with solvent. Other groups have recently described how simulations in H_2O can give new insights into the dynamic behavior of peptides. DiCapua et al.²⁴ documented in some detail the breaking of a single hydrogen bond occurring in a polyalanine helix solvated in H_2O ; there is however no control situation or an experimental system to closely match the origin of the destabilization in this system. While this work was in progress, Tirado-Rives and Jorgensen²³ described the simulation of an analogue of the ribonuclease S peptide at two different temperatures. They obtained a different helical content of the peptide for these two situations, in nice agreement with experiment. They did not however describe in detail the water–peptide interactions occurring during the unfolding. Here we also document some features of a solvated α -helical peptide, where the different stability in another solvent is used as a control. Some of these observations are in close agreement with those made by others, using slightly different procedures or different parameters

in their potential energy function describing the system.

As we performed this control simulation in TFE, it is reasonable to conclude that the observed unfolding is caused by the mere presence of the water molecules and is not an artifact of the simulation methodology used (e.g., the way the simulation is initiated or nonconservation of energy caused by nonbonded energy truncation). We observed the transient presence of the $i-i+3$ hydrogen-bonding pattern during the unfolding events of the peptide. In addition, we noted a general increase of the probability of finding this type of hydrogen bond at the end of helices, and this in both simulations. It seems therefore likely that the formation of this type of alternative hydrogen bond plays an important role in the formation and/or unfolding of any α -helix. This information may be of interest for the procedures used in the refinement stages of both NMR and X-ray structure determinations.

It is generally agreed upon that the propagation of helical structure in an already existing α -helical peptide is an energetically less demanding task when compared to the formation of the first turn of the α -helix.^{40,41} The unfolding of a peptide would therefore most probably also be a sequential process initiated once, for example, at the C-terminal end, and subsequently proceeding toward of the N-terminal end of the peptide. Although this general trend is observed here, there are noticeable exceptions that have their origin in stabilizing side chain-side chain interactions. The particular pathway of the helix-coil transitions is therefore not correctly described by a simple sequential change in pure ϕ - ψ dihedral angle space. Very subtle changes are involved, and the presence of different side chains clearly gives an individual nature to all transitions, as well as their sequential occurrence.

The formation, during unfolding, of a $i-i+3$ helical hydrogen-bonding pattern, followed by a series of turnlike conformations, described here as well as by others^{23,42} is in agreement with the

folding pathway proposed by Sunderalingam et al. based on the observations of water around helices in X-ray structures.³⁶ A single water molecule was observed inserting itself at the place of the $i-i+4$ hydrogen bond, as also described by DiCapua et al.²⁴ In addition, however, the analysis described here clearly shows that hydration of the hydrogen bond partners can also be mediated by different water molecules, as was observed by Tobias and Brooks⁴² during their free energy simulations of the initiation of a single helical turn. It seems therefore that both mechanisms can be involved in the same process, further underlining the individual nature of each transition.

What do we learn about the structure-promoting role of TFE versus H_2O ? From these simulations it is possible to argue that the different hydrogen-bonding characteristics of the water molecule and its different size are the only two factors needed to rationalize the differences with TFE. From the potential function and parameter set used in these simulations, together with the analysis presented in Figures 11 and 12, it is quite clear that hydrogen bonding between the carbonyl oxygens and solvent hydrogens is quite common in both simulations and is not helix destabilizing in itself. It is the inability of the TFE molecules, due to their size, to make the additional hydrogen bond with the amide proton that is probably the most determining factor.

In conclusion the data presented here show the possibilities of the molecular dynamics simulation technique to study protein unfolding (and folding) at the peptide level. Further analysis of this type will enable the elucidation of the detailed structural features of a solvated polypeptide, and its environment-structure relationships. This should facilitate the difficult task of rationalizing the actions of neuropeptides in general, and of galanin in particular, not only as a function of its structure at the target site, but also as a function of its structure in solution.

Acknowledgment. H.D.L. was supported by a Wenner-Grenn Foundation fellowship.

(40) Zimm, B. H.; Bragg, J. K. *J. Chem. Phys.* **1959**, *31*, 526-535.

(41) Schulz, G. E.; Schirmer, R. H. *Principles of Protein Structure*; Springer-Verlag: Berlin, 1979.

(42) Tobias, D. J.; Brooks, C. L., III. *Biochemistry* **1991**, *30*, 6059-6070.